Difference-of-Convex approach to chance-constrained Optimal Power Flow modelling the DSO power modulation lever for distribution networks

Ksenia Syrtseva, Welington de Oliveira, Sophie Demassey, Paul Javal, Hugo Morais, Bhargav Swaminathan

Highlights

Difference-of-Convex Approach to Chance-Constrained Optimal Power Flow modelling the DSO Power Modulation Lever for Distribution Networks

Ksenia Syrtseva,Welington de Oliveira,Sophie Demassey,Hugo Morais,Paul Javal,Bhargav Swaminathan

-
-
-

Difference-of-Convex Approach to Chance-Constrained Optimal Power Flow modelling the DSO Power Modulation Lever for Distribution Networks

Ksenia Syrtseva[a,b,*], Welington de Oliveira[b], Sophie Demassey[b], Hugo Morais[c], Paul Javal[a,b,1] and Bhargav Swaminathan[a]

[a]EDF R&D, 7, bd Gaspard Monge, Palaiseau, 91120, France
[b]Mines Paris, Université PSL, Centre de Mathématiques Appliquées (CMA), 1, rue Claude Daunesse, Sophia Antipolis, 06904, France
[c]Department of Electrical and Computer Engineering, INESC-ID—Instituto de Engenharia de Sistemas e Computadores-Investigação e Desenvolvimento, Instituto Superior Técnico (IST), Universidade de Lisboa, R. Alves Redol, 9, Lisbon, 1000-029, Portugal

ARTICLE INFO

Keywords:
Chance-constrained optimal power flow
Power modulation and curtailment
Difference-of-Convex
Uncertainty

ABSTRACT

The increasing expansion of renewable energy sources leads to the growth of uncertainty in the distribution network operation. Short-term operational planning performed by distribution system operators should evolve to address those new operating conditions, in particular to allow the efficient utilization of different flexibility levers. In this work, the use of a chance-constrained Alternating Current Optimal Power Flow (AC-OPF) is proposed to model the operational planning problem, considering the activation of several levers such as power modulation and power curtailment. The correlation between the renewable generation profiles and loads is taken into account via a joint probability constraint in the chance-constrained AC-OPF problem. The main novelty of the present manuscript is the adoption of a Difference-of-Convex approach that allows to solve the obtained optimization problem without convexification or linearization of the core OPF equations. The method starts with a reformulation of the model as a Difference-of-Convex optimization problem, and then a modified Bundle method algorithm is applied to solve it. The proposed methodology was tested in a 33 bus distribution network with 11 different values for the chance constraint satisfaction probability (safety parameter) ranging from 0.75 to 1.

1. Introduction

1.1. Context

The use of renewable energy sources (RES) is becoming increasingly important as the world seeks to transition to a more sustainable and environmentally friendly energy system. Several countries are proposing new targets to achieve carbon neutrality. For example, in Europe, several programs and initiatives have been defined such as *Green Deal*, *Fit to 55* or *RePower EU*. In all documents, the targets are becoming more and more ambitious with some concrete measures such as incentives for the development of renewables and the electrification of the transport sector [38]. Analysing with more detail the mentioned initiatives, it is clear that the transmission and distribution systems will be neuralgic infrastructures.

Feed-in tariffs (FiT) for RES production were one of the first incentive measures implemented by governments to encourage their development [55]. With these tariffs, RES production units could inject all the produced energy and receive fixed and economically attractive remuneration. Furthermore, system operators could not modulate the power injected by these units into their grid except under critical operation conditions. In practice, it implied that the system operators should be prepared to receive the contractualized capacity of production, which leads to significant investments in grid infrastructure. Depending on the circumstances, it resulted in a significant increase in cost for these producers, delays in commissioning, or even temporary limitations on the power injection during reinforcement works. Nowadays, considering the level of maturity of the RES technologies, mainly wind generation and solar photovoltaic, FiT have been replaced by other mechanisms [29]. Smart (and interruptible) connection points (SCP) and contracts have been proposed [1] for RES and are being implemented in Europe [12]. These contracts allow an increase in the hosting capacity of existing systems and thus faster integration of RES while reducing investment costs.

RES, such as solar and wind power, are inherently variable and intermittent, and therefore present significant challenges to the efficient and reliable operation of power systems. To address these challenges, system operators, mainly distribution system operators (DSOs), have to evolve from a traditional *fit and forget* approach in network planning and operation [16] to a more proactive one. Such a new approach involves optimization of multi-annual investments in human resources, infrastructure and technology, and the adoption of new methods and tools. In this context, many European DSOs are implementing a streamlined time-continuum based approach to network planning, operational planning

*Corresponding author
<ksenia-k.syrtseva@edf.fr> (K. Syrtseva);
<ksenia.syrtseva@minesparis.psl.eu> (K. Syrtseva)
ORCID(s): 0000-0003-2269-0228 (K. Syrtseva); 0000-0001-5906-4744 (H. Morais)
[1]Now at Enedis, Direction Technique, Departement Conduite, 26 rue de la Villette 69003 Lyon

and real-time operation, allowing a better and faster integration of new distributed energy resources (DER). This is, for example, highlighted in Enedis' (France's largest DSO) latest multi-annual network development plan [14]. Typically, this consists of characterising large investments several years in advance, identifying and prioritising medium-term investments, optimising works schedules in the short-term, and operating networks in an optimized fashion. This has however, and will continue to be, highly dependent on political decisions, as is the case with above-mentioned FiT and SCP mechanisms.

New network operational planning tools specifically tailored to these needs have already been deployed and are being improved to tackle the newest problems highlighted, for example, in [14]. These improvements include mathematical optimization based approaches to solving problems, which represent a complete shift in the operational planning paradigm for DSOs as it deals with the practical rules in use-cases and contractual obligations through mathematical optimization. DSOs like Enedis are continuing to work on deployment of newer methods that take into account other problems and opportunities like uncertainty in DER production, interaction with external actors (e.g. flexibility providers and TSOs), and integration of these new tools in their IT and OT systems.

These optimization methods rely on power flow equations in order to ensure technical constraint satisfaction. This, along with the objective of minimising costs associated with the operational solution, gives rise to an alternating-current optimal power flow problem (AC-OPF). In the case of the industrial optimization solution developed by Enedis, a deterministic and linearized AC-OPF model is used [44]. However, in a general case, an OPF problem is an optimization problem with mixed integer variables that is strongly NP-hard and nonconvex, as stated by various studies [7]. Several formulations and solution methods have been proposed [18, 37], including classical optimization methods that rely mainly on convex relaxations or approximations [30, 20], nondeterministic search techniques (also known as heuristic, stochastic or random search methods) [19], and machine learning methods [22].

1.2. Optimal Power Flow (OPF) under uncertainties

As traditional OPF models assume that the system parameters are deterministic, which may not be the case in practice [42], modelling uncertainties has become an important research topic in the field of electric power systems, particularly with the increasing penetration of RES. Solution methodologies of related optimization problems are diverse, and include meta-heuristic methods, robust and stochastic approaches. The former group has gained attention in the field of power and energy systems within the last ten years [8], due to the ability to search for near-optimal solutions in a large solution space efficiently (an overview of methods can be found in [34]). However, from a theoretical point of view, the quality of the obtained solution can be difficult to assess in practice, as no optimality certificate is provided.

Robust optimization methods rely on constructing an uncertainty set and searching for a reliable solution for any scenario realization. This approach is proposed for the management of distribution networks in [25, 17, 42, 53] with different types of uncertain data. For instance, uncertainties are solely on renewable energy sources in [25], whereas [53] deals with stochastic load composition. The authors in [42] describe multi-period grid management applying a convex hull technique to define an uncertainty set. Solutions obtained with robust optimization methods are optimal for the worst-case scenario, and thus tend to be conservative. In contrast, stochastic optimization methods assume that the probability distribution of uncertain variables is known [41, Chapter 1]. In particular, for the expected cost minimization framework, it allows to achieve (expected) minimal cost while preserving the required level of service for given scenarios. One widespread approach in stochastic programming is chance-constrained optimization, where one searches for a decision that minimizes costs while satisfying a set of random constraints with a prescribed probability level [41, 2]. Chance-constrained optimization models are intuitive and straightforward to explain. However, they are generally difficult to solve, because they often lack essential mathematical properties such as convexity and differentiability [46].

The use of chance (probability) constraints for energy management is discussed in detail in [50], where the authors show how to ensure feasibility to the greatest extent possible, while aligning with the goals of the system operator. In the framework of OPF problems, most chance-constrained models rely on linear or convex approximations and deal with individual probability constraints, i.e., correlations between random variables are ignored. In [54] an OPF problem with load uncertainties is considered, where probability constraints are represented with individual bounds on state variables. The model equations are linearized at the random vector expected value, establishing a monotonic relation between a constrained output and a random input. This fact enables to treat the probability constraints regarding the distribution of random variables. Partial linearization of power flow equations is applied in [39], in order to transform the individual chance constraints into deterministic ones at the forecasted operating point. One of the assumptions enabling the transformation is a relatively small forecast error on the model uncertainties. Another approximation is suggested in [10], where chance constraints are used to enforce voltage regulation with prescribed probability. The authors tackle them with convex relaxation and exploit linearization of load-flow equations. Reference [6] deals with minimization of an average generation cost over random renewable power injections, while controllable generators mitigate power fluctuations. To guarantee that thermal limits are exceeded with low probability and ensure that the generation remains within imposed bounds, chance constraints are employed separately for each type of constraint. Then,

the model is reduced to a deterministic convex optimization problem, more precisely, a second order cone program (SOCP). A SOCP reformulation is also used in [33, 5] for the case of individual chance constraints. In [31] a robust modification of the approach given in [6] is presented, which addresses the uncertainty in parameters of probability distributions by restricting them to an uncertainty set. Another robust reformulation of a chance-constrained OPF modelling systems with fluctuating power sources, is obtained in [52]. First, probabilistic bounds for the uncertainty are computed using scenario-based approach, and then a robust variant of the initial problem is solved due to these bounds.

A well-known downside of individual chance constraints is that they ignore the random vector correlations, which are important statistics that should be considered when modelling real-life problems. As a strong correlation between the renewable generation profiles and loads is observed [51, 36], in the present work, the OPF problem is modelled as a joint chance-constrained optimization problem. For a given parameter $\alpha \in [0, 1]$ and a probability measure $\mathbb{P}$, the problem we investigate in this work can be synthetized as follows:

$$\underset{\text{Levers}}{\textbf{min}} \quad \{ \text{ Levers activation cost } \} \tag{1a}$$

$$\text{s.t.} \quad \text{Activated levers satisfy contractual constraints} \tag{1b}$$

$$\mathbb{P}\left[\begin{array}{c}\text{Existence of a grid state within bounds}\\ \text{satisfying stochastic power-flow equations}\end{array}\right] \geq 1-\alpha. \tag{1c}$$

In this formulation, the decision variables are related to the activation of flexibility contracts (levers), which in our problem corresponds to DSO decisions on power modulation and power curtailment of distributed generation, and limitations on power supply to consumers (energy not supplied). Each grid user, who may be either a producer or a consumer, is characterized by its grid connection contract (FiT or SCP in our case). Depending on the contracts, levers activated by the DSO must satisfy specific deterministic constraints. Stochastic equations are related to technical decision feasibility: given a DSO decision and a scenario realization on power generation and loads, grid operating conditions must remain within technical limits. In practice, a decision on levers activation satisfying all the bounds and stochastic power flow equations for all the possible scenarios, may not exist. Hence, it makes sense to search for a reliable, affordable decision that satisfies the stochastic constraints with a probability level of at least $1-\alpha$. Observe that, if we take $\alpha = 0$ and a solution of problem (1) exists, then such a solution is robust over all the possible scenarios. The decision maker can thus adjust her risk aversion by appropriately setting the parameter α: small α reflects high risk aversion.

In the proposed approach, the primary goal is to secure the required level $1-\alpha$, with $\alpha > 0$, for the system: we search for an implementable decision that is feasible with a probability of at least $1-\alpha$. As we will see shortly, the goal is obtained without any stringent assumption on the probability distribution or modelling simplifications such as linearization and convexification of core OPF equations. The deterministic case $\alpha = 0$ is not within the scope of the proposed methodology, which is applicable but not tailored for this case. In section 2, we propose a realistic mathematical model for (1) that is consequently nonconvex, nondifferentiable, and thus challenging. Nonconvexity comes from the OPF equations, whereas the requirement under probability sign in (1c) causes nondifferentiability of the problem.

Despite recent advances in theory and numerical methods for chance-constrained problems, dealing with multivariate probability functions in optimization problems generally remains a challenging task. The main difficulty arises in evaluating the probability function and computing its (sub)gradient with reasonable precision. We recall that evaluating the probability function amounts to computing numerically a multidimensional integral, a very difficult task for even moderate dimensions [47]. The situation becomes even more demanding for assessing (sub)gradients. For this reason, a common practice is to estimate the probability function with Monte-Carlo simulations using a finite sample of scenarios [35]. For moderate sizes of the sample, and under the assumption that all involved functions are convex, one may model the probability constraint (1c) by using binary variables and `BigM` formulations (see, for instance, [49] and references therein). Such an approach is inappropriate for an OPF problem, because involved functions are not convex. Hence, without modelling simplifications, new mathematical approaches are required to face nonconvexity and nondifferentiability in problem (1). Based on the observation that the requirement under the probability in (1c) can be written as the difference of two convex functions, we apply a Difference-of-Convex (DoC)[1] optimization approach to tackle our problem. To the best of our knowledge, DoC programming has not yet been applied to the OPF class of problems.

1.3. Chance-constrained optimization and the DoC approach

A function is called DoC if it is expressible as the difference of two convex functions. As already investigated in [24] and [48], probability functions can be approximated as accurately as one wishes by DoC functions. In Subsection 3.1, it is shown how to model (without approximation) the existence requirement in (1c) by a DoC function. Therefore, we end up with a composition of DoC functions that is itself DoC, and thus we can approximate probability constraint (1c) with a DoC constraint:

$$\begin{aligned}\mathbb{P}\left[\begin{array}{c}\text{Existence of a grid state within bounds}\\ \text{satisfying stochastic power-flow equations}\end{array}\right] \geq 1-\alpha\\ \approx \quad c_1(x) - c_2(x) \leq 0,\end{aligned}$$

[1] The standard abbreviation for Difference-of-Convex is DC. To avoid confusion with "Direct Current" in OPF problems, we refer to the former as DoC.

where $c_1, c_2 : \mathbb{R}^n \to \mathbb{R}$ are (nondifferentiable) convex functions. Given this approximation, we will show how to construct a DoC optimization model for problem (1) fitting into the following general structure:

$$\min_{x \in X} f(x) := f_1(x) - f_2(x) \tag{2a}$$

$$\text{s.t. } c(x) := c_1(x) - c_2(x) \leq 0, \tag{2b}$$

where X is a nonempty bounded polyhedron contained in $\mathbb{R}^n$ and $f_1, f_2 : \mathbb{R}^n \to \mathbb{R}$ are convex functions as well. In the present work, we will refer to (2) as a DoC optimization problem.

DoC programming forms an important subfield of nonconvex programming, as it covers a large class of nonconvex optimization problems from real-life applications. At the same time, convex analysis apparatus enables to establish optimality conditions for DoC problems and design algorithms to solve them. These facts explain the increasing interest in this field, which started in the 80s [28]. Important facts about DoC programming such as optimality conditions and duality can be found in the tutorial paper [11]. The survey article [28] gives a large spectrum of examples and algorithm developments in this field. Currently, most used algorithms are based on iterative linearizations of components f_2 and c_2 [28], on penalization technique applied to the DoC constraint [27], and on improvement functions that combine constraint and objective in single level [48]. The latter is a well-known and successful strategy in the nonsmooth optimization literature [40, 3, 32, 48]. In particular, a bundle method with improvement function is proposed in [48] for dealing with DoC-constrained DoC-problems. Due to its good numerical performance reported in [48], we choose this bundle algorithm – denoted by DoC bundle method – to tackle our DoC optimization model (2) of the chance-constrained OPF problem (1).

1.4. Paper Structure and Contributions

The main contributions of the present paper are:

1. The formulation of the operational planning problem considering the activation of flexibility contracts (levers) under uncertainties, related to the probabilistic nature of nodal generation and consumption, as a joint chance-constrained OPF. The correlations among the random variables are thus taken into account. Furthermore, no model linearization or convexification is considered.
2. The design of an *oracle* (black-box) enabling to find a DoC decomposition of the constraint under probability sign, which imposes the OPF solution to be in the required bounds. This allows to apply DoC bundle method to the obtained chance-constrained OPF.
3. An illustration of the practical performance of DoC approach on two use-cases.

The remainder of this paper is organized as follows. Section 2 is dedicated to the modelling of short-term operational planning on grid users power modulation under uncertainties as a chance-constrained OPF. A reformulation of the obtained problem as a DoC model is given in Section 3, followed by an explanation of DoC bundle method. In Section 4, numerical results for two use cases are provided, which illustrate the performance of the described method.

2. Chance-constrained OPF model

In what follows the chance-constrained OPF model is described by setting the decision variables, state variables and constraints. The employed notation is introduced along the way.

2.1. Decision variables and random vector

We denote by $\mathcal{N}$ the set of buses of the grid, and by $\mathcal{A}$ the set of lines. Among the end buses $\mathcal{N}$, there is one slack bus and other buses with at most one connected grid user. Each grid user is either a producer or a consumer. The set of all grid users is denoted by $\tilde{\mathcal{N}} \subset \mathcal{N}$, identifying a grid user $i \in \tilde{\mathcal{N}}$ with a corresponding bus $i \in \mathcal{N}$. Let $\mathcal{G}$ and $\mathcal{L}$ be the subsets of producers and consumers, respectively. We wish to determine the active power p_i (positive for generation and negative for consumption) and reactive power q_i of each grid user $i \in \tilde{\mathcal{N}}$, based on the following decomposition:

$$p_i = p_i^{\phi}(\xi) - \boldsymbol{p}_i^{\gamma} - \boldsymbol{p}_i^{\nu}, \quad q_i = q_i^{\phi}(\xi) - \boldsymbol{q}_i^{\gamma} - \boldsymbol{q}_i^{\nu}. \tag{3}$$

For buses $i \in \mathcal{N} \setminus \tilde{\mathcal{N}}$ with no grid users, excluding the slack bus, we set $p_i = q_i = 0$. The active and reactive power demand (production and consumption), $p_i^{\phi}(\xi)$ and $q_i^{\phi}(\xi)$, are the *uncertain parameters* of our model, given as scenario realizations of a random vector $\xi \in \Xi \subset \mathbb{R}^d$. In case of considered flexibility contracts, the decision bears on the active power modulation for SCP grid users within the bounds of their guaranteed power denoted by $\boldsymbol{p}_i^{\gamma}$; on the active power curtailment for FiT grid users and SCP grid users beyond the bounds of their guaranteed power, and on limitations on power supply to consumers (energy not supplied), denoted by $\boldsymbol{p}_i^{\nu}$. We introduce also pair variables for reactive power modulation: $\boldsymbol{q}_i^{\gamma}$ for SCP grid users within the bounds of their guaranteed power; $\boldsymbol{q}_i^{\nu}$ for FiT grid users and SCP grid users beyond the bounds of their guaranteed power, and consumers. In fact, each reactive power variable is a function from the active, which will be defined in Subsection 2.3. This formulation was chosen as an easily modifiable for the case of other DSO levers, where the reactive power can be modulated directly. As the decision must be taken before scenario realization is known, the aforementioned decision variables do not depend directly on ξ. In order to distinguish different types of decision variables, we denote by $\mathcal{N}_{SCP}$ the set of indexes for $\boldsymbol{p}^{\gamma}$ and $\boldsymbol{q}^{\gamma}$, and by $\mathcal{N}_{FiT}$ that for $\boldsymbol{p}^{\nu}$ and $\boldsymbol{q}^{\nu}$ (note that $\mathcal{N}_{SCP} \subset \mathcal{G}$ and $\mathcal{L} \subset \mathcal{N}_{FiT}$). To simplify the notation, if there is no need to distinguish user types, we will denote decision variables by

$$\mathbf{p} := (\{\boldsymbol{p}_i^{\gamma}\}_{i \in \mathcal{N}_{SCP}}, \{\boldsymbol{p}_i^{\nu}\}_{i \in \mathcal{N}_{FiT}}) \in \mathbb{R}^n$$

$$\mathbf{q} := (\{\boldsymbol{q}_i^{\gamma}\}_{i \in \mathcal{N}_{SCP}}, \{\boldsymbol{q}_i^{\nu}\}_{i \in \mathcal{N}_{FiT}}) \in \mathbb{R}^n$$

with $n = |\mathcal{N}_{SCP}| + |\mathcal{N}_{FiT}|$.

On the contrary, the state variables $|V_i|$ and δ_i representing voltage at bus $i \in \mathcal{N}$, as well as p_{sb} and q_{sb} representing active and reactive power at slack bus, directly depend on ξ: once the scenario realization ξ is known, as well as the active and reactive power p_i and q_i for all $i \in \tilde{\mathcal{N}}$, state variables can be found by Gauss-Seidel, Newton-Raphson or similar methods [21].

Our problem thus has two main types of variables. First, the power modulation variables $\mathbf{p}_i$ and $\mathbf{q}_i$ are determined for all $i \in \mathcal{N}_{SCP} \cup \mathcal{N}_{FiT}$ before realization of the uncertain event. Then, after a scenario ξ is observed, which defines the power production and consumption, $p_i^{\phi}(\xi)$ and $q_i^{\phi}(\xi)$ for each grid user $i \in \tilde{\mathcal{N}}$, a new grid-state is determined. It is defined by the values of $|V_i|$ and δ_i, $i \in \mathcal{N}$, and p_{sb}, q_{sb}. The goal is to check whether an operational current transit (for a given scenario and power modulation) exists. In the next two subsections, we will detail how these two types of variables are combined in our chance-constrained OPF.

2.2. Power flow constraints under probability sign

We impose operational constraints which include bounds on voltage variables and constraints on the slack bus power variables. More specifically, we denote upper and lower bounds on voltage variables by $\overline{|V_i|}, \overline{\delta_i}$ and $\underline{|V_i|}, \underline{\delta_i}$, respectively. Constraints on active and reactive power at slack bus p_{sb} and q_{sb}, are represented by a set $\mathcal{F}_{sb}$ defined in Demand Connection Code [9], Figure 1. In addition, we add thermal constraints on current transit (congestion constraints): for each line (i, j) belonging to the set $\mathcal{A}$, we impose an upper limit $(I_{i,j}^{\max})^2$ on a quadratic form l from the current.

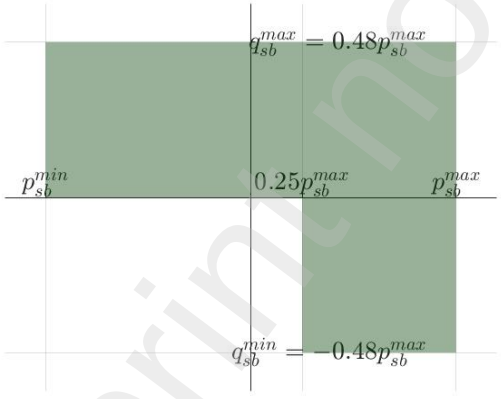

Figure 1: Feasible *P-Q* diagram for slack-bus following Demand Connection Code.

All in all, we get the following set of constraints:

$$\underline{\delta_i} \le \delta_i \le \overline{\delta_i}, \quad \forall i \in \mathcal{N} \tag{4a}$$

$$\underline{|V_i|} \le |V_i| \le \overline{|V_i|}, \quad \forall i \in \mathcal{N} \tag{4b}$$

$$l(|V_i|, |V_j|, \delta_i, \delta_j) \le (I_{i,j}^{\max})^2, \quad \forall (i,j) \in \mathcal{A} \tag{4c}$$

$$(p_{sb}, q_{sb}) \in \mathcal{F}_{sb}. \tag{4d}$$

In order to ease the model representation, let us define the following functions (here the sum is taken over all buses k connected to the bus i):

$$\begin{aligned} L_i^R(\mathbf{p}, \delta, |V|, \xi) :=& \\ \left(p_i^{\phi}(\xi) - \boldsymbol{p}_i^{\gamma} - \boldsymbol{p}_i^{\nu}\right) &+ \sum_{k\sim i} Y_{i,k}^R |V_i||V_k| \cos(\delta_i - \delta_k) \\ &+ \sum_{k\sim i} Y_{i,k}^I |V_i||V_k| \sin(\delta_i - \delta_k) \\ L_i^I(\mathbf{q}, \delta, |V|, \xi) :=& \\ \left(q_i^{\phi}(\xi) - \boldsymbol{q}_i^{\gamma} - \boldsymbol{q}_i^{\nu}\right) &+ \sum_{k\sim i} Y_{i,k}^R |V_i||V_k| \sin(\delta_i - \delta_k) \\ &- \sum_{k\sim i} Y_{i,k}^I |V_i||V_k| \cos(\delta_i - \delta_k). \end{aligned}$$

Such functions define the stochastic power flow equations of our problem.

We can now mathematically state the requirements under the probability sign in problem (1) by defining the following random set

$$X(\xi) := \left\{ (\mathbf{p}, \mathbf{q}) \;\middle|\; \begin{array}{c} \text{there exist } |V|, \delta, p_{sb}, q_{sb} \text{ satisfying (4)}, \\ L_i^R(\mathbf{p}, \delta, |V|, \xi) = 0 \;\text{ for all } i \in \mathcal{N}, \\ L_i^I(\mathbf{q}, \delta, |V|, \xi) = 0 \;\text{ for all } i \in \mathcal{N}. \end{array} \right\} \tag{5}$$

Note that variables $|V|, \delta, p_{sb}, q_{sb}$ depend directly on the random event ξ, whereas $(\mathbf{p}, \mathbf{q})$ must be decided before realization of ξ. We are thus interested in finding a decision $(\mathbf{p}, \mathbf{q})$ belonging to the random set $X(\xi)$ with probability $1 - \alpha$, which is represented by a probability constraint in our optimization model.

2.3. Chance-constrained OPF formulation

We continue by defining deterministic constraints of the problem. We start with the conservative bound on generation and consumption

$$\begin{aligned} \bar{p}_i^{\phi} &:= \min_{\xi \in \Xi} p_i^{\phi}(\xi) \quad \text{for all } i \in \mathcal{G} \\ \bar{p}_i^{\phi} &:= \max_{\xi \in \Xi} p_i^{\phi}(\xi) \quad \text{for all } i \in \mathcal{L}. \end{aligned}$$

When the support set of the random vector ξ is represented by finitely many Monte-Carlo scenarios, Ξ is a finite set, and thus computing $\bar{p}_i^{\phi}$ is a straightforward task. This parameter enters in our optimization problem bounding the decision variables on active power curtailment and modulation, p^{ν} and p^{γ}. The power curtailment must satisfy both contractual and technical bounds, for all realizations of the random vector ξ. Hence, we set the following constraints :

$$\begin{aligned} 0 \le \boldsymbol{p}_i^{\nu} \le \bar{p}_i^{\phi} \text{ and } \boldsymbol{q}_i^{\nu} = \tan\phi_i \boldsymbol{p}_i^{\nu}, \; i \in \mathcal{N}_{FiT} \cap \mathcal{G} \\ \bar{p}_i^{\phi} \le \boldsymbol{p}_i^{\nu} \le 0 \text{ and } \boldsymbol{q}_i^{\nu} = \tan\phi_i \boldsymbol{p}_i^{\nu}, \; i \in \mathcal{N}_{FiT} \cap \mathcal{L}. \end{aligned}$$

where parameter $\tan\phi_i$ is given for each grid user. Meanwhile, for $i \in \mathcal{N}_{SCP}$, the bounds on power modulation are determined contractually. They can be modelled as fractions of installed or subscribed power (for producer and consumer, respectively). Due to the data used in practice, we implemented them as a fraction of $\bar{p}_i^{\phi}$. All in all, we obtain the following constraints:

$$a_- \bar{p}_i^{\phi} \le \boldsymbol{p}_i^{\gamma} \le a_+ \bar{p}_i^{\phi} \quad \text{and} \quad \boldsymbol{q}_i^{\gamma} = \tan\phi_i \boldsymbol{p}_i^{\gamma},$$

with $a_- \in [-1, 0]$ and $a_+ \in [0, 1]$.

As for the objective function, we consider the case when $f(\mathbf{p}, \mathbf{q})$ is convex, Subsection 4.3. However, our approach remains valid as long as the objective function is DoC only using a generalized version of the algorithm proposed in [48].

Based on the assumptions described in the previous paragraphs, it is now possible to present the chance-constrained model for the considered stochastic OPF problem:

$$\min_{\mathbf{p},\mathbf{q}} \ f(\mathbf{p}, \mathbf{q}) \tag{6a}$$

$$\text{s.t. } 0 \le \boldsymbol{p}_i^{\nu} \le \bar{p}_i^{\phi} \quad \forall i \in \mathcal{N}_{FiT} \cap \mathcal{G} \tag{6b}$$

$$\bar{p}_i^{\phi} \le \boldsymbol{p}_i^{\nu} \le 0 \quad \forall i \in \mathcal{N}_{FiT} \cap \mathcal{L} \tag{6c}$$

$$\boldsymbol{q}_i^{\nu} = \tan\phi_i \boldsymbol{p}_i^{\nu}, \quad \forall i \in \mathcal{N}_{FiT} \tag{6d}$$

$$a_- \bar{p}_i^{\phi} \le \boldsymbol{p}_i^{\gamma} \le a_+ \bar{p}_i^{\phi}, \quad \forall i \in \mathcal{N}_{SCP} \tag{6e}$$

$$\boldsymbol{q}_i^{\gamma} = \tan\phi_i \boldsymbol{p}_i^{\gamma}, \quad \forall i \in \mathcal{N}_{SCP} \tag{6f}$$

$$\mathbb{P}\big[(\mathbf{p}, \mathbf{q}) \in X(\xi)\big] \ge 1 - \alpha. \tag{6g}$$

3. DoC reformulation and Bundle method

In this section, we first propose a DoC model for problem (6), and then we show how to solve it by the bundle method of [48]. The proposed model is built upon two DoC reformulations: one exact for the mathematical requirement $(\mathbf{p}, \mathbf{q}) \in X(\xi)$ and another approximate for the probability measure $\mathbb{P}$, as detailed in Subsections 3.1 and 3.2. Subsection 3.3 recalls the main details of the chosen optimization algorithm for solving the underlying problem.

3.1. DoC reformulation of the condition $(\mathbf{p}, \mathbf{q}) \in X(\xi)$

Let $\xi \in \Xi$ be fixed. For notational convenience, we will denote the decision variables $(\mathbf{p}, \mathbf{q})$ of our problem by $x \in \mathbb{R}^{2n}$. Our development starts by noting that the squared distance function to $X(\xi)$, i.e.,

$$d^2_{X(\xi)}(x) := \min_{z \in X(\xi)} \frac{1}{2}\|z - x\|^2,$$

yields the following useful relation:

$$x := (\mathbf{p}, \mathbf{q}) \in X(\xi) \quad \Longleftrightarrow \quad d^2_{X(\xi)}(x) = 0, \quad x \in \mathbb{R}^{2n}.$$

The squared distance function is not convex as the set $X(\xi)$ given in (5) is not convex. However, it is a DoC function as the following development shows:

$$\begin{aligned} d^2_{X(\xi)}(x) &= \min_{z \in X(\xi)} \left\{ \frac{1}{2}\|x\|^2 - \langle z, x\rangle + \frac{1}{2}\|z\|^2 \right\} \\ &= \frac{1}{2}\|x\|^2 - \max_{z \in X(\xi)} \left\{ \langle z, x\rangle - \frac{1}{2}\|z\|^2 \right\} \\ &= g_1(x, \xi) - g_2(x, \xi). \end{aligned}$$

Indeed, for any arbitrary ξ fixed, the convexity of both functions

$$g_1(x, \xi) := \frac{1}{2}\|x\|^2 \tag{7a}$$

$$g_2(x, \xi) := \max_{z \in X(\xi)} \left\{ \langle z, x\rangle - \frac{1}{2}\|z\|^2 \right\} \tag{7b}$$

with respect to x directly results from the definition of convexity. Moreover, observe that $g_1 - g_2$ is non-negative. As a result, we have the following DoC reformulation for checking whether $(\mathbf{p}, \mathbf{q})$ satisfies the constraints in (5):

$$x = (\mathbf{p}, \mathbf{q}) \in X(\xi) \quad \Longleftrightarrow \quad g_1(x, \xi) - g_2(x, \xi) \le 0.$$

While g_1 is a simple quadratic function, $g_2(\cdot, \xi)$ is more involved: it is the optimal value of a nonconvex optimization problem and is thus nondifferentiable. Its subdifferential at a given point x is given by

$$\begin{aligned} \partial g_2(x, \xi) := \Big\{ & s_2(\xi) \in \mathbb{R}^{2n} : \ g_2(z, \xi) \ge \\ & g_2(x, \xi) + \langle s_2(\xi), z - x\rangle \ \ \forall\, z \in \mathbb{R}^{2n} \Big\} \\ = \ & \arg\max_{z \in X(\xi)} \left\{ \langle z, x\rangle - \frac{1}{2}\|z\|^2 \right\} \\ = \ & \arg\min_{z \in X(\xi)} \frac{1}{2}\|z - x\|^2. \end{aligned}$$

If the set $X(\xi)$ were convex (and closed), then the above projection problem would have had a unique solution and, thus, g_2 would have been differentiable.

Note that evaluating g_2 at a given point x and computing one of its subgradient (an element of the subdifferential) amounts to projecting x onto the set $X(\xi)$ given in (5). This task can be accomplished (at least approximately) by OPF tools because this projection problem is indeed an OPF with a quadratic objective function. A numerical procedure (oracle) for accessing the DoC function $g_1(x, \xi) - g_2(x, \xi)$ and its first-order information is as follows. Here, we use the notation $(\mathbf{p}^k, \mathbf{q}^k)$ to highlight that this point is fixed, conceivably given by an algorithm at its iteration k.

Oracle 1. *Black-box for the DoC function* $g_1(x, \xi) - g_2(x, \xi)$.

1: *Given* $(\mathbf{p}^k, \mathbf{q}^k) \in \mathbb{R}^{2n}$ *and event/scenario* $\xi \in \Xi$, *let* $(\tilde{\mathbf{p}}, \tilde{\mathbf{q}})$ *be a solution of the OPF*

$$\min_{(\mathbf{p},\mathbf{q}) \in X(\xi)} \frac{1}{2}\|(\mathbf{p}, \mathbf{q}) - (\mathbf{p}^k, \mathbf{q}^k)\|^2, \quad \textit{with } X(\xi) \textit{ given in (5)}$$

2: *Set* $g_1(\mathbf{p}^k, \mathbf{q}^k, \xi) \leftarrow \frac{1}{2}\|\mathbf{p}^k\|^2 + \frac{1}{2}\|\mathbf{q}^k\|^2$ *and* $s_1^k(\xi) \leftarrow \begin{pmatrix} \mathbf{p}^k \\ \mathbf{q}^k \end{pmatrix}$

3: *Set* $g_2(\mathbf{p}^k, \mathbf{q}^k, \xi) \leftarrow \langle \mathbf{p}^k, \tilde{\mathbf{p}}\rangle - \frac{1}{2}\|\tilde{\mathbf{p}}\|^2 + \langle \mathbf{q}^k, \tilde{\mathbf{q}}\rangle - \frac{1}{2}\|\tilde{\mathbf{q}}\|^2$ *and* $s_2^k(\xi) \leftarrow \begin{pmatrix} \tilde{\mathbf{p}} \\ \tilde{\mathbf{q}} \end{pmatrix}$

4: *Return the first order information* $(g_1(\mathbf{p}^k, \mathbf{q}^k, \xi), s_1^k(\xi))$ *and* $(g_2(\mathbf{p}^k, \mathbf{q}^k, \xi), s_2^k(\xi))$.

The most time-consuming task in Oracle 1 is Step 1. To compute $(\tilde{\mathbf{p}}, \tilde{\mathbf{q}})$, we may employ standard solvers from the OPF literature and leverage computational burden by first checking whether $(\mathbf{p}^k, \mathbf{q}^k)$ satisfies the constraints in (5). The latter amounts to solving a system of load-flow equations and verifying if the computed solution $(\delta, |V|, p_{sb}, q_{sb})$ satisfies the bounds in (4). If it is the case, then $(\mathbf{p}^k, \mathbf{q}^k)$ automatically solves the OPF of Step 1: there is no need for calling an OPF solver, but only a (simpler) load-flow algorithm. However, if the computed solution of the load-flow equations does not satisfy (4), then we say that $(\mathbf{p}^k, \mathbf{q}^k)$ is infeasible for the future event ξ. In this case, an OPF solver must be applied to compute a point $(\tilde{\mathbf{p}}, \tilde{\mathbf{q}})$ that is feasible for the scenario ξ and as close as possible to $(\mathbf{p}^k, \mathbf{q}^k)$. Such a step thus amounts to answering the following question: given that $(\mathbf{p}^k, \mathbf{q}^k)$ is infeasible for scenario ξ,

> what is the smallest necessary perturbation on $(\mathbf{p}^k, \mathbf{q}^k)$ to render it feasible?

The answer is $(\tilde{\mathbf{p}}, \tilde{\mathbf{q}}) - (\mathbf{p}^k, \mathbf{q}^k)$, which is nothing but the opposite direction to the subgradient $s_1^k(\xi) - s_2^k(\xi)$. This fact explicitly reveals the practical role of the subgradients computed by Oracle 1: it guides the optimization process to seek for a better candidate solution (at the next iteration), and the use of an efficient OPF solver allows to improve numerical performance. However, caution is necessary: in this analysis, the oracle only sees the given individual scenario ξ. It is thus necessary to account for all the scenarios and the probability measure in a higher-level oracle. That is the goal in the following subsection.

3.2. DoC reformulation of probability constraint

This subsection aims at presenting a DoC approximation for the probability constraint (6g). From the previous subsection we have

$$\mathbb{P}[(\mathbf{p}, \mathbf{q}) \in X(\xi)] \quad \equiv \quad \mathbb{P}[g_1(\mathbf{p}, \mathbf{q}, \xi) - g_2(\mathbf{p}, \mathbf{q}, \xi) \leq 0],$$

with g_1, g_2 two convex functions given in (7). Hence,

$$\mathbb{P}[(\mathbf{p}, \mathbf{q}) \in X(\xi)] \geq 1 - \alpha$$

is equivalent to

$$\mathbb{P}[g_1(\mathbf{p}, \mathbf{q}, \xi) - g_2(\mathbf{p}, \mathbf{q}, \xi) > 0] \leq \alpha.$$

Next, we follow the lead of [48] to approximate the probability measure by a DoC function. To this end, let $v(\xi) = g_1(\mathbf{p}, \mathbf{q}, \xi) - g_2(\mathbf{p}, \mathbf{q}, \xi)$ be the random variable of interest, $\mathbb{E}[\cdot]$ the expected value operator w.r.t. $\mathbb{P}$, and let $\mathbf{1}_{(0,\infty)}(\cdot)$ denote the *characteristic function* of the segment $(0, \infty)$, that equals to 1 if $v > 0$, and 0 if $v \leq 0$. Recall that the following useful equivalence:

$$\mathbb{P}[v(\xi) > 0] \;=\; \mathbb{E}[\mathbf{1}_{(0,\infty)}(v(\xi))].$$

The main source of difficulties is that $\mathbf{1}_{(0,\infty)}(\cdot)$ is not convex and, even worse, it is discontinuous at 0. As in [24] and [48], we now approximate the characteristic function by a DoC one. Given a small parameter $t > 0$, the discontinuous characteristic function can be approximated by the continuous one

$$\zeta^t(v) := \begin{cases} 0, & \text{if } v \leq 0 \\ \frac{v}{t}, & \text{if } 0 < v \leq t \\ 1, & \text{if } t < v. \end{cases} \tag{8}$$

Observe that $\lim_{t \downarrow 0} \zeta^t(v) = \mathbf{1}_{(0,\infty)}(v)$ and $\zeta^t(v)$ has the following DoC decomposition:

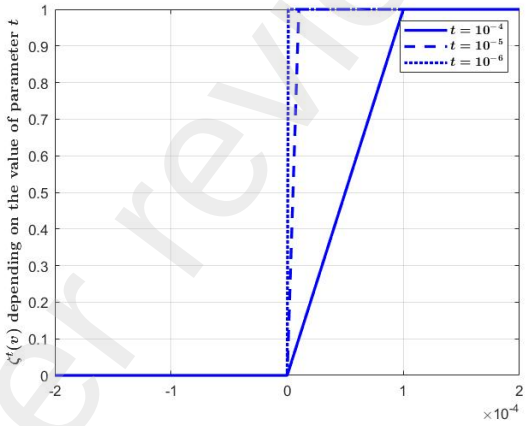

Figure 2: Function $\zeta^t(v)$ for $t = 10^{-4}$, $t = 10^{-5}$ and $t = 10^{-6}$.

$$\zeta^t(v) = \max\left\{\frac{v}{t}, 0\right\} - \max\left\{0, \frac{v-t}{t}\right\}.$$

Hence, the following expected value

$$\mathbb{E}[\zeta^t(g_1(\mathbf{p}, \mathbf{q}, \xi) - g_2(\mathbf{p}, \mathbf{q}, \xi))]$$

is an approximation of the probability

$$\mathbb{P}[g_1(\mathbf{p}, \mathbf{q}, \xi) - g_2(\mathbf{p}, \mathbf{q}, \xi) > 0].$$

Such approximation is as good as one wishes: the smaller is the parameter $t > 0$, the closer $\zeta^t(\cdot)$ is to $\mathbf{1}_{(0,\infty)}(\cdot)$. Furthermore, the composition of DoC functions under the expectation is itself a DoC function:

$$\zeta^t(g_1(\mathbf{p}, \mathbf{q}, \xi) - g_2(\mathbf{p}, \mathbf{q}, \xi)) = \frac{\max\{g_1(\mathbf{p}, \mathbf{q}, \xi), g_2(\mathbf{p}, \mathbf{q}, \xi)\}}{t} + 1 - \frac{\max\{g_1(\mathbf{p}, \mathbf{q}, \xi), g_2(\mathbf{p}, \mathbf{q}, \xi) + t\}}{t}.$$

It is well-known that the expectation $\mathbb{E}[\cdot]$ can be efficiently approximated via Monte-Carlo simulation by considering a fixed sample of scenarios randomly generated according to the distribution of ξ. As usual in the stochastic programming literature, in our numerical experiments we randomly generate a sample of N scenarios $\Xi := \{\xi^1, \dots \xi^N\}$ and estimate the convex functions

$$\mathbb{E}\left[\frac{\max\{g_1(\mathbf{p}, \mathbf{q}, \xi), g_2(\mathbf{p}, \mathbf{q}, \xi)\}}{t}\right] + 1$$

and $\mathbb{E}\Big[\dfrac{\max\{g_1(\mathbf{p},\mathbf{q},\xi), g_2(\mathbf{p},\mathbf{q},\xi)+t\}}{t}\Big]$.

by their sample average approximations. The justification of such an approach is well documented in the literature (e.g., [35]), and specialized to the the DoC setting in [24] and [26, Subsection 7.7.2]. Hence, we can approximate the probability constraint (6g) with the following DoC constraint

$$c_1(\mathbf{p},\mathbf{q}) - c_2(\mathbf{p},\mathbf{q}) \leq 0,$$

where

$$\begin{cases} c_1(\mathbf{p},\mathbf{q}) := \dfrac{1}{N}\displaystyle\sum_{j=1}^{N} \max\{g_1(\mathbf{p},\mathbf{q},\xi^j), g_2(\mathbf{p},\mathbf{q},\xi^j)\} \\ \qquad\qquad +t(1-\alpha), \\ c_2(\mathbf{p},\mathbf{q}) := \dfrac{1}{N}\displaystyle\sum_{j=1}^{N} \max\{g_1(\mathbf{p},\mathbf{q},\xi^j), g_2(\mathbf{p},\mathbf{q},\xi^j)+t\} \end{cases} \tag{9}$$

are convex functions. As a result, we have our DoC optimization model for the chance-constrained problem (6):

$$\begin{cases} \min\limits_{(\mathbf{p},\mathbf{q})\in X} & f(\mathbf{p},\mathbf{q}) \\ \text{s.t.} & c_1(\mathbf{p},\mathbf{q}) - c_2(\mathbf{p},\mathbf{q}) \leq 0, \end{cases} \tag{10a}$$

where

$$X := \{(\mathbf{p},\mathbf{q}) \in \mathbb{R}^{2n} : \ (6b)-(6f)\} \tag{10b}$$

is a polyhedral set. As discussed in Subsection 1.3, this optimization problem fits the structure of (2), and we can apply the DoC bundle method of [48] to tackle it.

3.3. DoC Bundle method

We start by highlighting that oracles for the functions in problem (10) are readily available. Indeed, f is a convex function and thus simple. Furthermore, an oracle for c_1 and c_2, providing their values and first-order information, is readily implementable thanks to Oracle 1 and assumption that we have finitely many N scenarios to represent the future random events: given $x := (\mathbf{p},\mathbf{q}) \in X$, an oracle provides $(c_1(x), s_1 \in \partial c_1(x))$ and $(c_2(x), s_2 \in \partial c_2(x))$. Note, however, that such an oracle is not a straightforward one: it requires calling Oracle 1 N times for the same $x = (\mathbf{p},\mathbf{q})$ given. In other words, N deterministic OPF (or load-flow problem) must be solved by Oracle 1 to compute (via (9) the function values and a pair of subgradients for c_1 and c_2.

Given these oracles, we can go further and briefly present the solving methodology, which has many numerical advantages: it does not require a feasible initial point, does not need penalty parameters, and numerical experience suggests that the approach is likely to escape bad-quality critical points. The interested reader is referred to [48] for a detailed presentation of DoC bundle method, as well as its mathematical properties. In that paper, the algorithm is given for a general case of DoC objective function, while the version presented below is adapted for convex objective. We start with the *improvement function* definition, an essential tool for presenting the algorithm:

$$H_{\hat{\tau}}(x) = \max\{f(x) - \hat{\tau}_f, c_1(x) - c_2(x) - \hat{\tau}_c\}. \tag{11}$$

In this definition, $\hat{\tau} \in \mathbb{R}^2$ is a parameter. The best choice for its value is $\hat{\tau} = (f^*, 0)$, with f^* the optimal value of (10): in this case, any solution of the problem $\min_{x\in X} H_{\hat{\tau}}(x)$ solves (10). However, as f^* is unknown we update $\hat{\tau}$ iteratively as follows: given $\hat{x} \in X$, a candidate point to solve (10) produced by the algorithm, we set

$$\hat{\tau} := (\hat{\tau}_f, \hat{\tau}_c) = (f(\hat{x}) + \rho \max\{c(\hat{x}), 0\},\ \sigma \max\{c(\hat{x}), 0\}), \tag{12}$$

where $\rho > 0$ and $\sigma \in [0, 1)$ can be freely chosen. The DoC bundle algorithm can be depicted as in Algorithm 1.

Algorithm 1 DoC bundle method

1: Given $x^0 \in X$, $\alpha \in [0,1]$, choose $\mu > 0$ and $\kappa \in (0,1)$. Set $\hat{x} \leftarrow x^0$ and $\hat{\tau}$ as in (12)
2: Compute $(f(x^0), s_f^0 \in \partial f(x^0))$ and $(c_i(x^0), s_i^0 \in \partial c_i(x^0))$, $i = 1, 2$
3: **for** $k = 0, 1, 2 \ldots$ **do**
▷ Trial point
4: Let x^{k+1} be the x-part solution of the quadratic program

$$\begin{cases} \min\limits_{x\in X, r\in\mathbb{R}^4} & r_4 - \langle s_2^k, x\rangle & + & \frac{\mu}{2}\|x-\hat{x}\|^2 \\ \text{s.t.} & f(x^j) + \langle s_f^j, x - x^j\rangle & \leq r_1, & j = 0,\ldots,k \\ & c_1(x^j) + \langle s_1^j, x - x^j\rangle & \leq r_2, & j = 0,\ldots,k \\ & c_2(x^j) + \langle s_2^j, x - x^j\rangle & \leq r_3, & j = 0,\ldots,k \\ & r_1 + r_3 - \hat{\tau}_f & \leq r_4 & \\ & r_2 - \hat{\tau}_c & \leq r_4 & \end{cases}$$

▷ Stopping test
5: **if** $\|x^{k+1} - \hat{x}\| \leq$ `Tol` **then**
6: Stop and return $\hat{x}$
7: **end if**
▷ Oracles call
8: Compute $(f(x^{k+1}), s_f^{k+1} \in \partial f(x^{k+1}))$ and $(c_i(x^{k+1}), s_i^{k+1} \in \partial c_i(x^{k+1}))$, $i = 1, 2$
▷ Descent test
9: **if** $H_{\hat{\tau}}(x^{k+1}) \leq H_{\hat{\tau}}(\hat{x}) - \kappa\frac{\mu}{2}\|x^{k+1} - \hat{x}\|^2$ **then**
10: Set $\hat{x} \leftarrow x^{k+1}$ and update $\hat{\tau}$ as in (12).
11: **end if**
12: **end for**

We highlight that Algorithm 1 is a simplified version of the one presented in [48]. For instance, the prox-parameter $\mu > 0$ can be updated iteratively, the number of constraints in the quadratic (master) program can be kept bounded, and the objective function can be DoC. The convergence analysis given in [48, Section 4] ensures that, under certain

conditions, Algorithm 1 provides a critical point (i.e., a point satisfying necessary optimality conditions) of problem (2).

4. Results

4.1. Network

The current research study utilizes a medium voltage distribution network, inspired by [4, 43], consisting of 33 buses, accommodating 31 loads and with a total peak consumption of approximately 16.6 MW. The network incorporates three distributed generation (DG) units, comprising two biomass plants (one with SCP contract connected in bus 12 with an installed capacity of 6.97 MW and another with FiT contract connected in bus 29 with an installed capacity of 3.86 MW), and one wind farm with a FiT contract connected in bus 32 with an installed capacity of 0.47 MW. The network is connected to the high-voltage network in bus 1 which is considered the slack bus in the present study. The consumption and generation values were defined to have the network operating near by their technical limits creating the need for flexibility activation. The schematic representation of the network is illustrated in Figure 3.

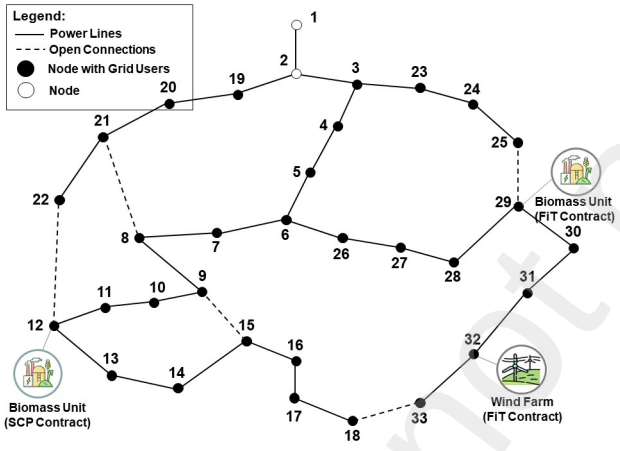

Figure 3: Medium voltage distribution network, 32 buses.

4.2. Scenario generation

In order to test the proposed DoC approach on the test network described in Subsection 4.1, we use Enedis Open Data [15] on July 27, 2020, to construct load and generation profiles for $N = 1000$ scenarios. Three types of grid users are considered: biomass generation, wind generation and consumption (data based on small and medium enterprises). For each grid user $i \in \mathcal{N}$, we denote the provided data by $(\tilde{p}_i^{\phi}, \tilde{q}_i^{\phi})$. Next, we attribute an individual variance σ_i^2: 0.0248 for biomass generation type, 0.01 for wind generation type, and 4 different values in the range between $6.01 \cdot 10^{-5}$ and 0.01 for consumers. Consider covariance matrix Σ with $\Sigma_{i,j} = r_{i,j}\sigma_i \cdot \sigma_j$, where $r_{i,j} = 1$ if the types of users i and j coincide, and 0 otherwise; and normalization matrix A with $A_{i,j} = 0.5$ if the user $i = j$ is a generator, $A_{i,j} = 5000$ if the user $i = j$ is a consumer, and 0 otherwise. Applying the procedure described in [23], we calculate the nearest symmetric positive semi-definite matrix $\tilde{\Sigma}$ to $A\sigma$. Finally, we generate vectors p^{ϕ} and q^{ϕ} following multivariate Gaussian distributions with the means $\tilde{p}^{\phi}$ and $\tilde{q}^{\phi}$, respectively, and covariance $\tilde{\Sigma}$.

4.3. Parameters of DoC approach

Here and in what follows $P_{base} = 1\,\text{MW}$, $V_{base} = 12.66\,\text{kV}$ and $I_{base} = 78.99\text{A}$.

The upper and lower bounds in (4b) are defined in the network design manual of a French DSO [13, Annex 1.3] specifically related to connection contracts for grid users, and represent ±5% of nominal voltage for MV network. The upper and low bounds on δ in (4a) are set to $\pm\frac{\pi}{2}$. For all $(i,j) \in \mathcal{A}$, thermal constraints (4c) are reduced to $|I_{i,j}|^2 \leq (I_{i,j}^{\max})^2$. In order to simplify computations of Oracle 1, we use a convexification of the feasible set $\mathcal{F}_{sb}$ in (4d), Figure 1. Such a convexification is defined by

$$S = \left\{ (p_{sb}, q_{sb}) \in \mathbb{R}^2 : p_{sb}^{\min} \leq p_{sb} \leq p_{sb}^{\max}, \right.$$
$$q_{sb}^{\min} \leq q_{sb} \leq q_{sb}^{\max},$$
$$\left. q_{sb} \geq \frac{-0.48 p_{sb}^{\max}}{-p_{sb}^{\min} + 0.25 p_{sb}^{\max}} p_{sb} + \frac{0.48 p_{sb}^{\max} p_{sb}^{\min}}{-p_{sb}^{\min} + 0.25 p_{sb}^{\max}} \right\}.$$

and corresponds to the union of green and blue sets on Figure 4.

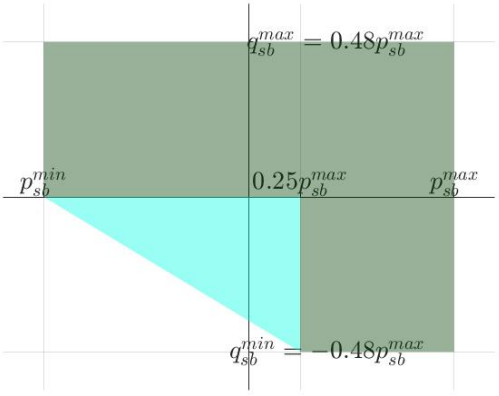

Figure 4: Convexification of the feasible set for slack-bus constraint.

The objective function is convex and has the following structure (all the coefficients are non-negative):

$$f(\mathbf{p}, \mathbf{q}) = f_1(\mathbf{p}) + f_2(\mathbf{p}), \tag{13a}$$

where

$$f_1(\mathbf{p}) = \sum_{i \in \mathcal{N}_{SCP}} C_{SCP}^i |p_i^{\gamma}|$$
$$+ \sum_{i \in \mathcal{N}_{FiT} \cap \mathcal{G}} C_{FiT,g}^i |p_i^{\nu}| + \sum_{i \in \mathcal{N}_{FiT} \cap \mathcal{L}} C_{FiT,l}^i |p_i^{\nu}| \tag{13b}$$

Table 1
Coefficients in the objective function (13) for each grid user (GU).

GU	Contract	Type	Coeff. in $f_1(\mathbf{p})$	Coeff. in $f_2(\mathbf{p})$
12	SCP	Biomass generation	$4.2 \cdot 10^{-5}$	0
12, 29	FiT	Biomass generation	$4.2 \cdot 10^{-3}$	0.01
32	FiT	Wind generation	0.02	0.1
Others	FiT	Consumption	1	1

and

$$f_2(\mathbf{p}) = \sum_{i \in \mathcal{N}_{SCP}} c^i_{SCP}(p^\gamma_i)^2 + \sum_{i \in \mathcal{N}_{FiT} \cap \mathcal{G}} c^i_{FiT,g}(p^\nu_i)^2 + \sum_{i \in \mathcal{L}} c^i_{FiT,l}(p^\nu_i)^2. \quad (13c)$$

The values of coefficients in (13b) and (13c) are given in Table 1. Our motivation for this choice is as follows. First, the component $f_1(\mathbf{p})$ reflects the cost of levers activation (since coefficients in Table 1 are set as dimensionless quantities, this cost is expressed in pu). As power modulation of a FiT producer is more expensive compared to that of a SCP grid user, the inequality [2] $C^i_{FiT,g} \gg C^j_{SCP}$ should be respected for $i, j \in \mathcal{G}$. Moreover, as limitation on power supply to a consumer is more expensive than power curtailment of producer, the inequality $C^i_{FiT,l} \gg C^j_{FiT,g}$ should be satisfied for $i, j \in \mathcal{N}_{FiT}$. Thus, the following relation $C^i_{FiT,l} \gg C^j_{FiT,g} \gg C^k_{SCP}$ is respected in (13b). Further, as penalty for the energy not supplied is defined by a regulator, we set $C^i_{FiT,l} = C^j_{FiT,l}$ for all consumers $i, j \in \mathcal{L}$. Since the contracts may differ depending on generation technology, we fix different coefficients for biomass generation and wind generation. Meanwhile, the quadratic terms are introduced as a penalty that encourages fairness in power modulation among the same types of users, as the minimum in (13c) is attained at a point where activation of levers is equal among grid users with equal coefficients. Thus, we set $c^i_{FiT,l} = c^j_{FiT,l}$ for $i, j \in \mathcal{N}_{FiT}$, i.e. we impose the coefficients to be equal for FiT consumers. We also assume that the quadratic coefficients are equal among FiT producers of the same generation type.

Unless otherwise specified, the approximation parameter t from (8) is set to 10^{-5}. The choice of parameters in DoC Bundle method [48] is as follows: $\rho = 10^7$, $\sigma = 0.5$, $\kappa = 0.9$, $\delta_{Tol} = 10^{-7}$, $\mu_{\min} = 10^{-6}$ and $\mu_{\max} = 10^6$. To test the performance of the presented DoC approach for the chance-constrained problem (6), we set 11 values of safety parameters $1 - \alpha$ ranging from 0.75 to 1 with a step size of 0.025 (the case $\alpha = 0$ is tested as an extreme one, the algorithm is not designed for deterministic framework). We consider two cases: one where only voltage constraints are detected (buses 9, 10, 11, 15, 16 and 17) in initial state of the grid, i.e. without levers activation, and another with an additional congestion constraint. For the second case, we set an upper limit on current for the line connecting buses 2 and 19. The constraint value is chosen in such a way that it is violated for 533 scenarios in initial state of the grid (without levers activation).

[2] The relation "$a \gg b$" means that a is much greater than b.

4.4. Case 1: Voltage constraints

For each value of safety parameter, the algorithm manages to find a feasible critical point with average execution time of 1665 seconds (in a personal laptop) ranging from 1059 ($1 - \alpha = 0.875$) to 2279 ($1 - \alpha = 0.775$) seconds. In order to check validation of the chance constraint, we compare targeted value of safety parameter with the ratio of scenarios satisfying load-flow equations. In initial state of the grid, without levers activation, the latter is equal to 0.545. After the optimization is performed, it gets close to targeted safety parameter with a tendency to approach it as the parameter increases, Figure 5. It remains below the targeted value due to approximation of probability function used for DoC formulation (see Subsection 3.2). Varying parameter t that participates in DoC approximation of probability constraint (see eq. (8)), $t = 10^{-4}, 10^{-5}$ and 10^{-6}, for a fixed safety parameter value $1 - \alpha = 0.9$, the ratio of scenarios satisfying load-flow equations becomes 0.839, 0.876 and 0.893, respectively. This illustrates, as expected, an increase in accuracy as t goes to zero.

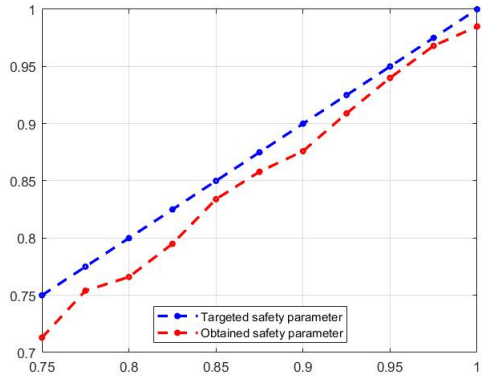

Figure 5: Comparison of targeted safety parameter $1 - \alpha$ with the obtained one (for t=10^{-5}).

The volume of active power modulation grows linearly up to $1 - \alpha = 0.925$ and accelerates afterwards, as illustrated in Figure 6. The same tendency is valid for the volume supplied by FiT grid users, whose share in total power curtailment remains within $69 - 77\%$. Meanwhile, a SCP grid user supplies the remaining part of the volume within the bounds of her guaranteed power for all values of safety parameter. Power modulation cost, represented by (13b) in the objective function, follows the same upward trend as power modulation volume. It is consistent with the price formation, which is in linear dependence on the latter.

Therefore, a slight decrease in safety parameter implies a reduction in total cost of power modulation. This result aligns with our expectations from probabilistic modelling of power flow constraints.

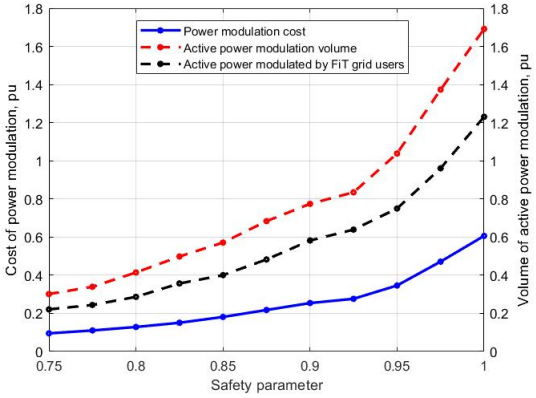

Figure 6: Cost and volume of power modulation.

Computing maximum and average amplitudes of constraint violation over all scenarios where constraint violations are detected, we compare them with average volume of power modulation supplied by one grid user. Without levers activation, the maximum amplitude of constraint violation is 0.0339 pu, whereas the average is 0.0057 pu. Figure 7 reveals a notable decrease in maximum amplitude of constraint violation for $1-\alpha > 0.825$ up to 0.0102 pu ($\alpha = 0$), and a significant growth in average volume of power modulation while increasing the system reliability. This confirms that the higher volume of levers is activated, the less amplitude of constraint violation is. To ensure the system reliability with $1-\alpha \geq 0.9$, average power modulation volume exceeds maximum amplitude of constraint violation. The gap between two figures drastically increases as $1-\alpha$ approaches 1 due to stochastic character of our problem: if we did not have to deal with uncertainties and the scenario realization was known, covering the maximum amplitude of constraint violation would have been sufficient.

Meanwhile, the average amplitude of constraint violation fluctuates near the value 0.0045 pu with a slight tendency to decrease. These upward and downward trends in amplitude of constraint violation lead to the following conclusions. More reliable but costly solutions cover risky scenarios which allow higher amplitude of constraint violation. At the same time, they tolerate those where constraint violation amplitude is closer to average. This result is based on simulations, and does not follow from chance-constrained formulation as it says nothing about amplitude of constraint violation. Moreover, this conclusion contradicts mathematical intuition that we would have had for a convex problem: maximum amplitude of constraint violation grows, as risky scenarios are more costly to cover.

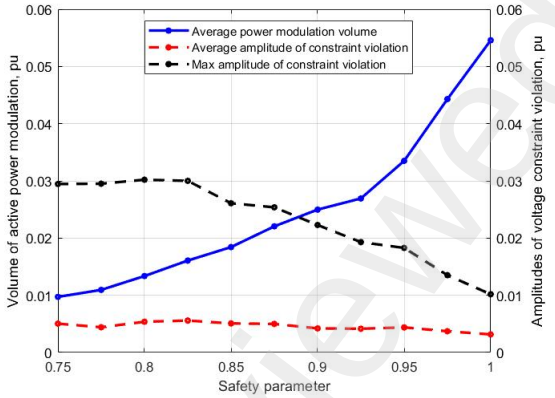

Figure 7: Volume of power modulation and amplitudes of constraint violation.

4.5. Case 2: Voltage and congestion constraints

The algorithm finds a critical point with average execution time of 1947 seconds ranging from 1353 ($1-\alpha = 0.85$) to 2850 ($1-\alpha = 0.825$) seconds. However, for deterministic case $\alpha = 0$, the algorithm does not manage to find a feasible solution. The ratio of scenarios satisfying load-flow equations is equal to 0.266 for the initial state of the grid. As Figure 8 shows, the latter approaches the targeted value of safety parameter once levers activation is optimized. However, for $1-\alpha > 0.95$, the difference between targeted and obtained value of safety parameter increases. This can be due to the fact that a robust solution may not exist. The difference between targeted and obtained value of safety parameter represents 4.6% of targeted value for $\alpha = 0$, whereas, initially, it was only 3.4% for $1-\alpha = 0.75$. The gap for $\alpha = 0$ is significant due to infeasibility of obtained solution.

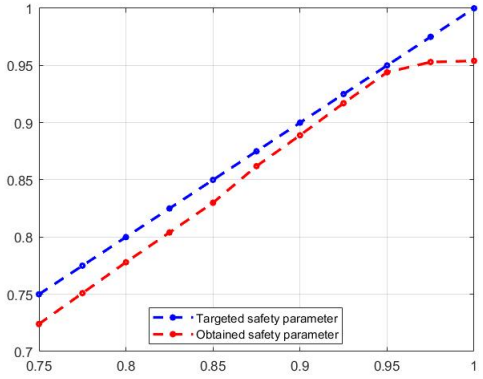

Figure 8: Comparison of targeted safety parameter $1-\alpha$ with the obtained one.

Similarly to the case without congestion constraint, power modulation cost repeats the growth dynamics of power modulation volume, Figure 9. The part supplied by FiT grid users constitutes from 79% to 87% of total volume, and the remaining part is due to a SCP grid user within the

bounds of her guaranteed power. However, compared to the previous case, the growth acceleration of power modulation cost and volume is less pronounced as safety parameter goes to 1. Moreover, these values become almost stable at $1-\alpha = 0.975$ and $\alpha = 0$, which is consistent with the fact that the corresponding number of covered scenarios is very close (953 for $1-\alpha = 0.975$ and 954 for $\alpha = 0$). Thus, except the deterministic case with $\alpha = 0$ when obtained solution is not feasible, a small decrease in safety parameter enables to reduce the total cost of levers activation.

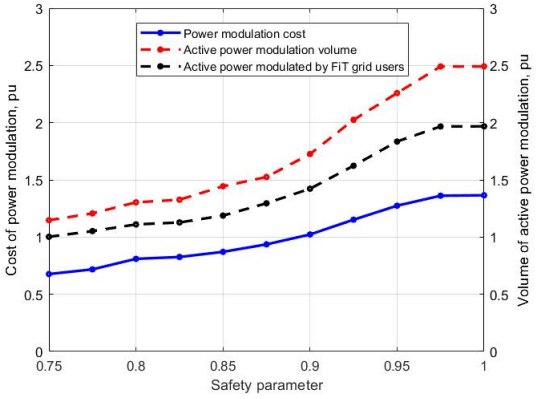

Figure 9: Cost and volume of power modulation.

As in the previous case, we compute average and maximum amplitudes of voltage constraint violation. These values are calculated over all scenarios where voltage constraint violation is detected (scenarios where only congestion constraint is violated, are not included). Without levers activation, they remain the same as in the case without congestion constraint. Meanwhile, maximum and average amplitudes of congestion constraint violation calculated over all scenarios where congestion constraint violation is detected, are 0.3851 pu and 1.5155 pu, respectively. As the order of magnitude of congestion constraint violation is greater than that of voltage constraint violation, the corresponding values are plotted separately, Figure 10 and Figure 11. All in all, they illustrate the same trends as in the previous case, namely, a steady decrease in maximum amplitude of constraint violation, both for voltage and congestion constraints. At the same time, Figure 10 reveals a significant growth in average volume of power modulation while increasing the system reliability. Thus, the conclusion that an increase in volume of levers activation reduces the amplitude of constraint violation, remains valid.

Comparing curves of average power modulation volume on Figure 7 and Figure 10, we observe that it is higher for the case with congestion constraint. Moreover, average power modulation volume always exceeds maximum amplitude of voltage constraint violation in the latter case. This is due to stochastic character of our problem, but also to additional amplitude of congestion constraint violation that should be covered by power modulation. Meanwhile, we see the opposite trend for the curves of maximum amplitude of

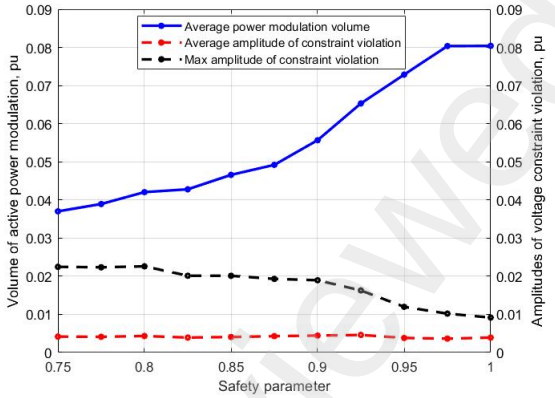

Figure 10: Volume of power modulation and amplitudes of constraint violation (excluding congestion constraint violation).

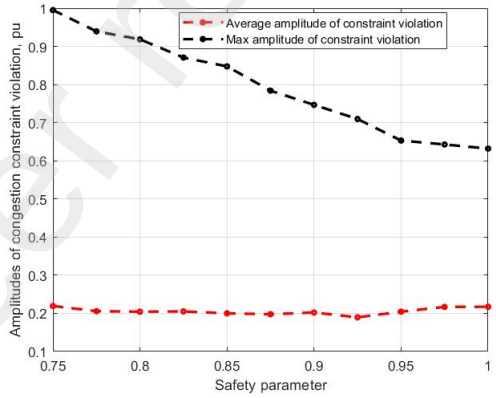

Figure 11: Amplitudes of congestion constraint violation.

constraint violation (without congestion constraint). It can be explained by the curtailment of grid users downstream of the congestion constraint for all values of safety parameter, which is aimed to cover an essential part of scenarios where congestion constraint is detected. This curtailment weakens voltage constraints at other buses of the grid, and reduces amplitude of their violation for not covered scenarios. Furthermore, the ratio of scenarios where congestion constraint is violated among all not covered scenarios, remains within $47-59\%$, and tends to slightly increase as safety parameter goes to 1. In other words, more reliable but costly solutions are more prone to cover scenarios without congestion constraints.

Comparing activation of levers for grid users downstream the line connecting buses 2 and 19 (congestion constraint in Case 2) in two considered use cases, we observe that there is no power curtailment of those grid users for all values of safety parameter $1-\alpha$, $\alpha > 0$ in Case 1. This result is coherent with the expectations, as they do not contribute to resolution of existing voltage constraints. Meanwhile, they are curtailed in Case 2 for all values of safety parameter $1-\alpha$, $\alpha > 0$. As the voltages constraints are the same in both use cases, we conclude that their curtailment resolve

only the congestion constraint. Moreover, we also observe that the power curtailment is not equal among those users, although all of them are consumers. Consequently, the soft constraint imposed by quadratic terms (13c) in the objective function, is not sufficient to force an equal power curtailment inside the same group of grid users. This is due to nonconvex nature of the optimization model.

5. Conclusion

This paper presented a novel formulation of the distribution network operational planning problem as a chance-constrained AC-OPF modelled using a DoC approach. This approach takes into account uncertainties related to nodal production and consumption, and proposes solutions to the chance-constrained problem through the activation of flexibility (power modulation) from SCP and FiT grid users. The solution methodology consists in model reformulation as a DoC optimization problem with the use of a special numerical procedure (oracle), and the subsequent use of DoC Bundle method. The main advantages of the employed approach are:

1. The joint probability constraint in the obtained chance-constrained OPF model allows to take into account correlation between RES generation profiles and load profiles.
2. The use of DoC approach enables to solve the optimization problem avoiding linearization and convexification of power flow equations.
3. The method allows to consider wide range of objective functions and constraints, as long as they can be represented as DoC functions. In particular, it can be applied for modelling other DSO levers, e.g. reactive power modulation.
4. Different OPF solvers/strategies can be employed in the oracle that computes function values and subgradients. Integration of an efficient solver improves the numerical performance of DoC Bundle method.

The perspectives of this work include application of a generalize version of DoC Bundle method presented in [45] for solving DoC reformulation of the chance-constrained OPF. From a theoretical point of view, this algorithm provides a solution satisfying stronger optimality condition, but has potentially lower computational efficiency as no explicit DoC decomposition of involved functions is used. Another perspective consists in adjusting the objective function and deterministic constraints of the model for the practical goals of the DSO, as the solution methodology gives a large spectre of options. However, the use of binary variable can be required for modelling some of DSO rules, for instance, an accurate requirement of the fairness in power modulation among the same types of grid users. For these cases, a modification of the solution methodology is necessary, as DoC Bundle method is adapted only for continuous variables.

6. Acknowledgements

W. Oliveira acknowledges financial support from the Gaspard-Monge Program for Optimization and Operations Research (PGMO) project "Scalable Optimization for Learning and Energy Management."

H. Morais was supported by Portuguese national funds through FCT, Fundação para a Ciência e a Tecnologia, under the project UIDB/50021/2020.

K. Syrtseva acknowledges financial support from EDF R&D for the PhD thesis work.

CRediT authorship contribution statement

Ksenia Syrtseva: Methodology, Software, Investigation, Visualization, Writing - Original Draft, Writing - Review Editing. **Welington de Oliveira:** Conceptualization, Methodology, Software, Visualization, Validation, Writing - Review Editing, Supervision. **Sophie Demassey:** Conceptualization, Methodology, Validation, Visualization, Writing - Review Editing, Supervision. **Hugo Morais:** Conceptualization, Visualization, Investigation, Validation, Writing - Review Editing, Supervision. **Paul Javal:** Methodology, Software, Investigation, Visualization. **Bhargav Swaminathan:** Conceptualization, Validation, Visualization, Writing - Review Editing, Supervision.

References

[1] Anaya, K.L., Pollitt, M.G., 2017. Going smarter in the connection of distributed generation. Energy Policy 105, 608–617. doi:https://doi.org/10.1016/j.enpol.2017.01.036.

[2] Ansaripour, R., Barati, H., Ghasemi, A., 2022. A chance-constrained optimization framework for transmission congestion management and frequency regulation in the presence of wind farms and energy storage systems. Electric Power Systems Research 213, 108712. doi:https://doi.org/10.1016/j.epsr.2022.108712.

[3] Apkarian, P., Noll, D., Rondepierre, A., 2008. Mixed H_2/H_∞ Control via Nonsmooth Optimization. SIAM Journal on Control and Optimization 47, 1516–1546.

[4] Baran, M., Wu, F., 1989. Network reconfiguration in distribution systems for loss reduction and load balancing. IEEE Transactions on Power Delivery 4, 1401–1407. doi:10.1109/61.25627.

[5] Bauer, R., Mühlpfordt, T., Ludwig, N., Hagenmeyer, V., 2023. Analytical uncertainty propagation for multi-period stochastic optimal power flow. Sustainable Energy, Grids and Networks 33, 100969.

[6] Bienstock, D., Chertkov, M., Harnett, S., 2014. Chance-constrained optimal power flow: Risk-aware network control under uncertainty. SIAM Review 56, 461–495. doi:10.1137/130910312.

[7] Bienstock, D., Verma, A., 2019. Strong NP-hardness of AC power flows feasibility. Oper. Res. Lett. 47, 494–501. doi:10.1016/j.orl.2019.08.009.

[8] Chicco, G., Mazza, A., 2020. Metaheuristic optimization of power and energy systems: Underlying principles and main issues of the 'rush to heuristics'. Energies 13. doi:10.3390/en13195097.

[9] Commission Regulation (EU), 2016. Network Code on Demand Connection DC. Technical Report. URL: https://eur-lex.europa.eu/legal-content/EN/TXT/?uri=uriserv%3AOJ.L_.2016.223.01.0010.01.ENG.

[10] Dall'Anese, E., Baker, K., Summers, T., 2017. Chance-constrained AC optimal power flow for distribution systems with renewables. IEEE Transactions on Power Systems 32, 3427–3438. doi:10.1109/TPWRS.2017.2656080.

[11] de Oliveira, W., 2020. The ABC of DC programming. Set-Valued and Variational Analysis 28, 679–706. doi:10.1007/s11228-020-00566-w.

[12] Decree, 2021. Arrêté du 12 juillet 2021 d'application de l'article D. 342-23 du code de l'énergie (*in French*). Technical Report. URL: https://www.legifrance.gouv.fr/jorf/id/JORFTEXT000043788443.

[13] Enedis, 2019. Principes d'étude et de développement du réseau pour le raccordement des clients consommateurs et producteurs BT (*in French*). Technical Report. URL: https://www.enedis.fr/media/2168/download.

[14] Enedis, 2023. Network Development Plan (*in French*). Technical Report. URL: https://enedisfr-bo.prod.web-enedis.fr/sites/default/files/documents/pdf/plan-de-developpement-de-reseau-document-preliminaire-2023.pdf.

[15] Enedis 2020, . Enedis open data. URL: https://data.enedis.fr/explore/dataset/coefficients-des-profils/table/?disjunctive.sous_profil&refine.horodate=2020. accessed: 2021-11-29.

[16] Fattaheian-Dehkordi, S., Tavakkoli, M., Abbaspour, A., Fotuhi-Firuzabad, M., Lehtonen, M., 2020. An incentive-based mechanism to alleviate active power congestion in a multi-agent distribution system. IEEE Transactions on Smart Grid 12, 1978–1988.

[17] Franco, J.F., Ochoa, L.F., Romero, R., 2018. AC OPF for smart distribution networks: An efficient and robust quadratic approach. IEEE Transactions on Smart Grid 9, 4613–4623. doi:10.1109/TSG.2017.2665559.

[18] Frank, S., Steponavice, I., Rebennack, S., 2012a. Optimal power flow: a bibliographic survey i. Energy Systems 3, 221–258. doi:10.1007/S12667-012-0056-Y.

[19] Frank, S., Steponavice, I., Rebennack, S., 2012b. Optimal power flow: a bibliographic survey ii. non-deterministic and hybrid methods. doi:10.1007/S12667-012-0057-X.

[20] Gan, L., Low, S.H., 2014. Convex relaxations and linear approximation for optimal power flow in multiphase radial networks , 1–9doi:10.1109/PSCC.2014.7038399.

[21] Grainger, J., Stevenson, W., 1994. Power System Analysis. McGraw-Hill Education. URL: https://books.google.fr/books?id=NBIoAQAAMAAJ.

[22] Hasan, F., Kargarian, A., Mohammadi, A., 2020. A survey on applications of machine learning for optimal power flow , 1–6doi:10.1109/TPEC48276.2020.9042547.

[23] Higham, N., 1988. Computing a nearest symmetric positive semidefinite matrix. Linear Algebra and Its Applications 103, 103–118. doi:10.1016/0024-3795(88)90223-6.

[24] Hong, L., Yang, Y., Zhang, L., 2011. Sequential convex approximations to joint chance constrained programed: A monte carlo approach. Operations Research 3, 617–630.

[25] Jabr, R.A., 2013. Adjustable robust OPF with renewable energy sources. IEEE Transactions on Power Systems 28, 4742–4751. doi:10.1109/TPWRS.2013.2275013.

[26] Javal, P., 2021. Integrating uncertainties in short-term operational planning. Ph.D. thesis. Mines-Paris, PSL.

[27] Le Thi, H.A., Ngai, H.V., Tao, P.D., 2014. DC programming and DCA for general DC programs, in: Van Do, T., Le Thi, H.A., Nguyen, N.T. (Eds.), Advanced Computational Methods for Knowledge Engineering: Proceedings of the 2nd International Conference on Computer Science, Applied Mathematics and Applications (ICCSAMA 2014). Springer International Publishing, pp. 15–35. doi:10.1007/978-3-319-06569-4.

[28] Le Thi, H.A., Pham Dinh, T., 2018. DC programming and DCA: thirty years of developments. Mathematical Programming 169, 5–68.

[29] Leiren, M.D., Reimer, I., 2020. Germany: From feed-in tariffs to greater competition, in: Comparative Renewables Policy. Routledge, pp. 75–102.

[30] Low, S.H., 2014. Convex relaxation of optimal power flow—part i: Formulations and equivalence. IEEE Transactions on Control of Network Systems 1, 15–27. doi:10.1109/TCNS.2014.2309732.

[31] Lubin, M., Dvorkin, Y., Backhaus, S., 2016. A robust approach to chance constrained optimal power flow with renewable generation. IEEE Transactions on Power Systems 31, 3840–3849. doi:10.1109/TPWRS.2015.2499753.

[32] Montonen, O., Joki, K., 2018. Bundle-based descent method for nonsmooth multiobjective DC optimization with inequality constraints. Journal of Global Optimization 72, 403–429.

[33] Mühlpfordt, T., Faulwasser, T., Hagenmeyer, V., 2018. A generalized framework for chance-constrained optimal power flow. Sustainable Energy, Grids and Networks 16, 231–242.

[34] Niu, M., Wan, C., Xu, Z., 2014. A review on applications of heuristic optimization algorithms for optimal power flow in modern power systems. Journal of Modern Power Systems and Clean Energy 2, 289–297. doi:10.1007/s40565-014-0089-4.

[35] Pagnoncelli, B.K., Ahmed, S., Shapiro, A., 2009. Sample average approximation method for chance constrained programming: Theory and applications. Journal of Optimization Theory and Applications 142, 399–416. doi:10.1007/s10957-009-9523-6.

[36] Qi, B., Hasan, K.N., Milanović, J.V., 2019. Identification of critical parameters affecting voltage and angular stability considering load-renewable generation correlations. IEEE Transactions on Power Systems 34, 2859–2869. doi:10.1109/TPWRS.2019.2891840.

[37] Qiu, Z., Deconinck, G., Belmans, R., 2009. A literature survey of optimal power flow problems in the electricity market context , 1–6doi:10.1109/PSCE.2009.4840099.

[38] Reinhilde Bouckaert, 2023. From the green deal to repower EU. URL: https://feps-europe.eu/wp-content/uploads/2023/02/From-the-Green-Deal-to-REPower-EU.pdf. accessed: 2023-05-13.

[39] Roald, L., Andersson, G., 2018. Chance-constrained AC optimal power flow: Reformulations and efficient algorithms. IEEE Transactions on Power Systems 33, 2906–2918. doi:10.1109/TPWRS.2017.2745410.

[40] Sagastizábal, C., Solodov, M., 2005. An infeasible bundle method for nonsmooth convex constrained optimization without a penalty function or a filter. SIAM Journal on Optimization 16, 146–169. URL: http://siamdl.aip.org/dbt/dbt.jsp?KEY=SJOPE8&Volume=16&Issue=1.

[41] Shapiro, A., Dentcheva, D., Ruszczyński, A., 2009. Lectures on Stochastic Programming: Modeling and Theory. MPS-SIAM Series on Optimization, SIAM - Society for Industrial and Applied Mathematics and Mathematical Programming Society, Philadelphia.

[42] Soares, T., Bessa, R., Pinson, P., Morais, H., 2017. Active distribution grid management based on robust AC optimal power flow. IEEE Transactions on Smart Grid PP, 1–1. doi:10.1109/TSG.2017.2707065.

[43] Sousa, T., Morais, H., Vale, Z., Faria, P., Soares, J., 2012. Intelligent energy resource management considering vehicle-to-grid: A simulated annealing approach. IEEE Transactions on Smart Grid 3, 535–542. doi:10.1109/TSG.2011.2165303.

[44] Swaminathan, B., Matthieu, A., Benoit, B., 2021. OptimGP - industrial optimisation for enedis' short-term operational planning. CIRED 2021 - The 26th International Conference and Exhibition on Electricity Distribution 2021, 1161–1165. doi:10.1049/icp.2021.1956.

[45] Syrtseva, K., de Oliveira, W., Demassey, S., van Ackooij, W., 2023. Minimizing the difference of convex and weakly convex functions via bundle method. URL: https://optimization-online.org/?p=21655. submitted.

[46] van Ackooij, W., 2020. A discussion of probability functions and constraints from a variational perspective. Set-Valued and Variational Analysis 28, 585 – 609. doi:10.1007/s11228-020-00552-2.

[47] van Ackooij, W., de Oliveira, W., 2014. Level bundle methods for constrained convex optimization with various oracles. Computational Optimization and Applications 57. doi:10.1007/s10589-013-9610-3.

[48] van Ackooij, W., Demassey, S., Javal, P., Morais, H., de Oliveira, W., Swaminathan, B., 2021. A bundle method for nonsmooth DC programming with application to chance-constrained problems. Computational Optimization and Application 78, 451–490. doi:10.1007/s10589-020-00241-8.

[49] van Ackooij, W., Frangioni, A., de Oliveira, W., 2016. Inexact stabilized benders' decomposition approaches with application to chance-constrained problems with finite support. Computational Optimization and Applications 65, 637–669.

[50] van Ackooij, W., Zorgati, R., Henrion, R., Möller, A., 2011. Chance Constrained Programming and Its Applications to Energy Management. doi:10.5772/15438.

[51] Verzijlbergh, R.A., De Vries, L.J., Lukszo, Z., 2014. Renewable energy sources and responsive demand. do we need congestion management in the distribution grid? IEEE Transactions on Power Systems 29, 2119–2128. doi:10.1109/TPWRS.2014.2300941.

[52] Vrakopoulou, M., Katsampani, M., Margellos, K., Lygeros, J., Andersson, G., 2013. Probabilistic security-constrained AC optimal power flow, in: 2013 IEEE Grenoble Conference, pp. 1–6. doi:10.1109/PTC.2013.6652374.

[53] Xu, Y., Ma, J., Dong, Z.Y., Hill, D.J., 2017. Robust transient stability-constrained optimal power flow with uncertain dynamic loads. IEEE Transactions on Smart Grid 8, 1911–1921. doi:10.1109/TSG.2015.2510447.

[54] Zhang, H., Li, P., 2011. Chance constrained programming for optimal power flow under uncertainty. IEEE Transactions on Power Systems 26, 2417–2424. doi:10.1109/TPWRS.2011.2154367.

[55] Zhao, G., Zhou, P., Wen, W., 2021. Feed-in tariffs, knowledge stocks and renewable energy technology innovation: The role of local government intervention. Energy Policy 156, 112453. doi:https://doi.org/10.1016/j.enpol.2021.112453.